

Aircraft Target Identification by Null Polarization Based Feature Set

Faisal Aldhubaib

Electronics Department, College of Technological Studies, Public Authority of Applied Education, Kuwait

Abstract: *The paper utilizes a small feature set formed by the polarization nulls of the target's resonances to identify airborne model targets. Once linked to the target resonances, the small feature set can reflect shape attributes like the elongation, symmetry, and tilt degrees in the individual target substructures. Based on a 3D feature space formed by these three degrees, the identification approach applies Euclidean distance measure to identify two electrically similar targets of similar resonance behavior. The identification performance indicated that the feature set is robust, and in particular, the elongation feature demonstrated superior discriminative ability.*

Keywords: Characteristics Polarization Theory, Radar Target Identification, Supervised Learning, Lagrangian Optimization

1. Introduction

As the need to identify radar targets accurately as either friendly or hostile at a distance in confrontational situations is essential to most defense applications, the function of the radar signal processing should involve actively classifying the targets categorically and then identify them individually. Such process of decision making often relies upon target recognition algorithms based on template matching or statistical models. Importantly, it is common to use the resonance frequency set, which in turn relates to the target dimensions, to categorize or classify it in the learning database and then use the target's shape to identify it. Henceforth, the classification then identification stages lead to computationally efficient target recognition methods. For targets of similar resonance set but different shape, then recognition is possible based on the shape attributes like symmetry, elongation, and tilt degrees. Such attributes inferred from characteristics polarization of the target as the target works like a transformer of the incident wave polarization. Henceforth, the incorporation of characteristics polarization states (CPS) with a radar signature is beneficial, e.g. [1-4], and will also enhance the target backscattering return; and subsequently, the ability to better identify radar targets even if the targets are of the same class category such as airborne targets, e.g. [5-8].

However, A full polarization information about the target individual structures requires the CPS set along the target dominant resonant frequencies. In this respective, the Singularity Expansion Model (SEM) [10] and the Method-Pencil-Function (MPOF) algorithm [11] come in handy. The SEM express the late-time portion of the backscattered signal as a sum of exponentially decaying signals of complex natural resonances (CNR), of course, with the assumption of sufficient broadband illumination of the target under test. The MPOF enables the estimation of the target CNR set from the backscattered late-time response even with low Signal-to-Noise ratio (SNR), where a CNR forms a minimal set of parameters to represent the target signature, i.e. the complex frequency and the associated strength, namely residue. Henceforth, a quadrature matrix of the orthonormal set of residues at a single resonance will carry information about an individual target structure. By applying a Lagrangian

optimization to the power terms, the second moments, a matrix of the residue with the antenna directions as Stokes variables, the optimum antenna directions (represented by four Stokes variables) for null reception can be found, and subsequently the required shape degrees [12].

For identification stage, the polarization angle set will form the variables of the feature space with their observations, i.e. samples, generated with a preset signal to noise ratio (SNR). To be able to identify a target, its associated angles should form recognizable and discriminable patterns in the feature space. As the pattern becomes more recognizable, the identification task will be simpler even with simple distance measures [13, 14]. Here, an observation or a sample is represented by a point in 3D space formed by the three shape degrees at a particular resonance frequency. Therefore, for each resonance, there will be a separate feature set to evaluate its respective identification performance. For given target conditions, we quantify the quality of identification as the probability or number of correct identification decisions as a function of the environment disturbance.

Hence, the new contribution of this paper is the evaluation of an identification algorithm based on the proposed polarization angle set, and in cases of fully and partially polarized wave. Section 2 presents the signal preprocessing steps, co-nulls derivation process, and then the identification approach. Section 3 shows the target model and the identification performances for a different set of shape degrees and resonances. Finally, section 4 reaches conclusions and point out the direction of further studies.

2. Method

Obtain the transient response by Fourier transforming the low-pass filtered frequency response with the filter's cutoff set above the highest resonance of interest. The calculation of a sufficiently broadband frequency response is made feasible by the method of moments using FEKO software [15]. Set the SNR level by adding Additive White Gaussian noise (AWGN) to the transient signal, then select the late-time onset after the specular response has vanished (approximately at twice the maximum target dimension L per speed of light c , i.e. $2L/c$). Apply the MPOF to the truncated late time

portion to extract the CNR. The late time signal $a(t)$ is represented by the SEM model as a sum or series of CNR as follows:

$$a(t) = \sum_{n=1}^M c_n e^{-(\sigma_n + j\omega_n)t} \quad (1)$$

Such that M , c , σ , and ω terms denote respectively the number of CNRs excited, the residue, the damping factor, and the frequency of the CNR mode. The extraction of a CNR is sensitive to noise and late-time onset selection, for this make sure the reconstructed signal resembles the original signal to a significant extent [16].

2.1 Co-null states

Typical preprocessing steps to derive the co-nulls are: For a CNR of interest, and for three polarization directions, i.e. two orthogonal co-polarization and one cross-polarization due to reciprocity, construct the 2x2 residue matrix for this particular CNR as follows [17]:

$$C = \begin{bmatrix} c_{xx} & c_{xy} \\ c_{yx} & c_{yy} \end{bmatrix} \quad (2)$$

Where subscripts xx and yy denote the co-polarization directions, and $xy=yx$ (due to reciprocity) denote the cross-polarizations directions. Then, establish the co-power equation with the second moments (Kronecker product) of the residue matrix C and the fictitious antenna in Stokes vector form g as follow:

$$P_c = \mathbf{g}^T \cdot \mathbf{A} \cdot (|[C] \otimes [C]^*|) \cdot \mathbf{A}^{-1} \cdot \mathbf{g} \quad (3)$$

Where $\mathbf{A} = \begin{pmatrix} 1 & 0 & 0 & 1 \\ 1 & 0 & 0 & -1 \\ 0 & 1 & 1 & 0 \\ 0 & j & -j & 0 \end{pmatrix}$ and $\mathbf{g} = [g_0 \ g_1 \ g_2 \ g_3]$

To derive the co-null states in Stokes variables terms $g_{1, 2, 3}$, solve simultaneously (by the Lagrangian optimization method) the three partial derivatives of the power equation in (3) as a function of the Stokes variables and the constraint condition Φ as follows:

$$\frac{\partial P_c}{\partial g_m} - \mu \frac{\partial \Phi}{\partial g_m} = 0, \quad m = 1, 2, 3. \quad (4)$$

Subject to $\Phi(g_1, g_2, g_3) = \sqrt{g_1^2 + g_2^2 + g_3^2} = P$, where $0 < P < 1$.

The P account for the loss of polarization degree in the wave polarization mainly due to noise. Theoretically, we can handle this loss with ensemble average, so that will not affect the computation of the estimated proposed angles if properly averaged.

Now, the two co-null states g_{cn1} and g_{cn2} are in the form of Stokes vector, such that:

- 1st. The elongation degree β (0-45°) is determined by taking the dot product of the null vectors as
 $\beta = 45^\circ - (45^\circ \times |g_{cn1} \cdot g_{cn2}|)$
- 2nd. The symmetry degree ε (0-45°) is determined from the g_3 sum of the two co-nulls as
 $\varepsilon = \frac{1}{2} \sin^{-1} (g_{3cn1} + g_{3cn2})$
- 3rd. The tilt degree τ (0-90°) is determined from the g_1 and g_2 of the two co-nulls as
 $\tau = \frac{1}{2} \tan^{-1} [(g_{2cn1} + g_{2cn2}) / (g_{1cn1} + g_{1cn2})]$

2.2 Identification process

Based on supervised learning approach, the identification process involves two modes of operations: (a) an off-line training mode to build the cataloged database and (b) real-time testing mode. In the training mode, use samples of the feature set of known candidate targets to construct the targets database. Then the testing mode involves deriving the feature set of an unknown target under observation and making a decision as to the identity of this unknown target. In general, decision-making includes determining the proximity (similarity) between a test sample and the cataloged database to declare the identity of the observed target, assuming the availability of the target measured in the database.

In this case, consider the shape degrees as the variables of the feature space for each resonance, in another word; select the angles as the dimensions of the feature space. Assuming known target aspect, keep the target's aspect constant such in the case of moving targets. In general, we will evaluate the identification performance by a pairwise distance measure of the unknown test sample to the corresponding estimated sample in stored in the training database. Hence, assign the unknown sample to the target with the minimum defined distance. The identification process includes two stages as follows:

Training stage:

- 1st. Preset the level of AWGN, generate N corrupted observations/samples of angles at each CNR. (In the testing stage, the same N samples are considered the test samples.)
- 2nd. Build the training database for each CNR by taking the ensemble average of its associated samples. (Thus the training samples are estimated with preset level of SNR.)
- 3rd. For stationary targets, repeat for all target aspect angles of interest (omitted in our case).

Testing stage:

- 4th. Generate a new sample or use the N samples from the training stage as the test samples.
- 5th. Expressed in degrees, measure the distance, e.g. Euclidian type, between the tested sample and the targets trained sample, i.e. estimated.
- 6th. Assign this sample to the target with the minimum aggregate distance accumulated across the angles and resonances of interest.

The results will then show how well the identification algorithm performs by counting the number of correct identification instances and expressing the result as a percentage of total trials.

3. Results

Figure 1 depicts the modeled aircraft, where the angle θ_r defines the rotation of the target longitudinal axis from the u_3 axis in a counterclockwise direction. The angles θ_w and θ_t represent the inclination degrees in the wing and the tail sections along the longitudinal axis. Figure 2 depicts the target sections current vs. frequency responses, which

provides a breakdown of the aircraft resonant frequencies (as indicated by the relevant peaks in the spectrum) and shows to which geometrical section a resonance belongs. In this case, the estimated resonance set is predominately at 150, 300, 410 and 490MHz corresponding respectively to the mid, nose-wing, wing and tail sections.

For comparison purpose, select two shape configurations A and B as listed in Table I. Figure 3 depicts a 2D feature space with only the tilt and the elongation angles as dimensions, here, the scatter plot forms a pool of 40-test sample generated with 5dB SNR. Generated with AWGN, the distribution is normal for the samples in the feature space, as expected. In the tilt dimension, as expected both targets A&B₄₅ reflect a tilt angle around 45° at all resonances, whereas target B₂₀ has a tilt angle around 20°. Figure 4 demonstrates the training samples estimated based on ensemble average of each pool of observations as depicted in Figure 3. These estimates will form the cataloged database in the training stage. Most distinctive feature is the elongation angle along the third and fourth resonances, which in turn is related to the wing and the tail sections, respectively. This distinctiveness coincides with the fact that the targets shapes differ in these two parts. Figure 5 gives an example of the distance calculated for 40 trials based on the symmetry angle associated with the fundamental resonance only. As mentioned earlier, this feature is redundant for this type of symmetrical targets, and as expected, its probability of correct identification is around 50%, i.e. random. Listed in Table II are the results of identification performances as per shape degrees and a different set of resonances. The symmetry, in this case, is the least distinctive feature, whereas the elongation angle has the highest probability of correct identification. Among the individual resonances, linked to the wings the third resonance is the most distinctive as the identification rate is the highest in general. Also, it is clear that combining the shape degrees and largely the resonance modes enhance the identification performance.

4. Conclusions

Even for a single and low-order resonance, the elongation feature has demonstrated superior identification ability for the same class case but with parts of different inclination degrees. Therefore, evaluating this polarization angle at the target resonances is most beneficial for decision-making. Also, the elongation angle is invariant with target orientation along the line of sight. In general, the distribution of observations in the feature space constructed by the symmetry, tilt, and elongation angles is straightforward and recognizable for the case of a simple wire target with a fixed aspect angle; therefore the decision algorithm such as distance learning was simple to implement and sufficient for this scenario or case. However, expect the complexity of decision-making algorithm to increase with unknown target aspect angle, e.g. buried or concealed target and the more is the structural complexity of the target. For further studies the following are considered; (a) the space diversity in the target aspect angle; (b) targets in half space, e.g. [18];(c)exploiting other algorithms of decision making like the nearest neighbor or even statistical methods, especially nonparametric types, e.g. [19].

References

- [1] D. A. Garren, A. C. Odom, M. K. Osborn, J. S. Goldstein, S. U. Pillai, and J. R. Guerci, "Full-polarization matched-illumination for target detection and identification, " *Aerospace and Electronic Systems*, IEEE Transactions on, vol. 38, pp. 824-837, 2002.
- [2] H. Mott, *Remote sensing with polarimetric radar* New York, N.Y: Wiley-IEEE; Chichester: John Wiley 2007.
- [3] C. E. Baum, "Combining Polarimetry with SEM in Radar backscattering for Target Identification, " *Invited Paper in Conference on Ultrawideband and Ultrashort Impulse Signals*, 18-22 September, Sevastopol, Ukraine, 2006.
- [4] D. Giuli, "Polarization diversity in radars, " *Proceedings of the IEEE*, vol. 74, pp. 245-269, 1986.
- [5] F. Aldhubaib and N. V. Shuley, "Radar Target Recognition Based on Modified Characteristic Polarization States, " *IEEE Transactions on Aerospace and Electronic Systems*, vol. 46, pp. 1921-1933, 2010.
- [6] FA Sadjadi, CSL Chun, A Sullivan, and G. Gaunard, "The Huynen-Fork Polarization Parameters in the Classification of Dielectric Mine-like Objects, " *Sensing and Imaging: An International Journal*, vol. 7, 2006.
- [7] W. C. Chen and N. V. Z. Shuley, "Robust Target Identification Using a Modified Generalized Likelihood Ratio Test, " *IEEE Transactions on Antennas and Propagation*, vol. 62, pp. 264-273, 2014.
- [8] H. S. Lui and N. V. Shuley, "Resonance Based Target Recognition Using Ultrawideband Polarimetric Signatures, " *IEEE Transactions on Antennas and Propagation*, vol. 60, pp. 3985-3988, 2012.
- [9] F. Aldhubaib, "Shape degreesAs A Radar Feature Set " *International Journal of Enhanced Research in Science Technology & Engineering (IJERSTE)*, vol. 5, April - 2016 2016.
- [10] C. E. Baum, E. J. Rothwell, K.-M. Chen, and D. P. Nyquist, "The singularity expansion method and its application to target identification, " *Proceedings of the IEEE*, vol. 79, pp. 1481-1492, 1991.
- [11] T. K. Sarkar and O. Pereira, "Using the matrix pencil method to estimate the parameters of a sum of complex exponentials, " *Antennas and Propagation Magazine*, IEEE, vol. 37, pp. 48-55, 1995.
- [12] F. Aldhubaib, N. V. Shuley, and H. S. Lui, "Characteristic Polarization States in an Ultrawideband Context Based on the Singularity Expansion Method, " *IEEE Geoscience and Remote Sensing Letters*, vol. 6, pp. 792-796, 2009.
- [13] R. O. Duda, P. E. Hart, and D. G. Stork, *Pattern Classification*, 2nd ed.: New York: Wiley, 2001.
- [14] A. K. Jain, R. P. W. Duin, and M. Jianchang, "Statistical pattern recognition: a review, " *Pattern Analysis and Machine Intelligence*, IEEE Transactions on, vol. 22, pp. 4-37, 2000.
- [15] E. s. a. Systems, "Feko Suit 5, " 9.3.24 ed. S.A (Pty) Ltd, 2003-2005.
- [16] F. Aldhubaib, "Validation of Shape degreesBased Resonance Modes, " *International Journal of Engineering Research and Applications*, vol. 6, pp. 57-61, May 2016.

[17] F. Aldhubaib, "Stability of Target Resonance Modes: In Quadrature Polarization Context, " International Journal of Engineering Research and Applications, vol. 6, pp. 39-42, May 2016.

[18] H. S. Lui, F. Aldhubaib, N. V. Z. Shuley, and H. T. Hui, "Subsurface Target Recognition Based on Transient

Electromagnetic Scattering, " IEEE Transactions on Antennas and Propagation, vol. 57, pp. 3398-3401, 2009.

[19] F. Aldhubaib, H. S. Lui, N. V. Shuley, and A. Al-Zayed, "Aspect segmentation and feature selection of radar targets based on the average probability of error, " IET Microwaves, Antennas & Propagation, vol. 4, pp. 1654-1664, 2010.

Table I: Targets A and B configurations.

Target	Rotation θ_r	Wing inclination θ_w	Tail inclination θ_t
A	45	30	60
B ₄₅	45	45	45
B ₂₀	20	45	45

Table II: Targets A&B identification Results for each polarization angle under 5dB SNR condition.

Resonance under test	Symmetry (ϵ)	Tilt (τ)	Elongation (β)
1	50	47.5	100
2	57.5	82.5	100
3	65	87.5	100
4	55	75	100
1&2	58	83	100
3&4	63	78	100
1, 2&3	60	90	100
All	60	95	100

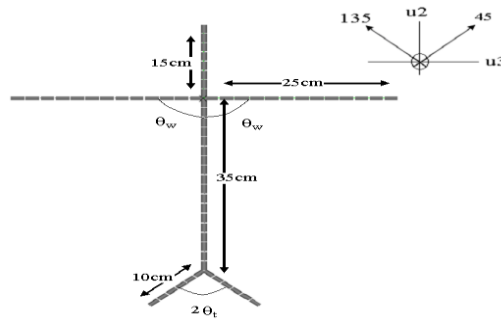


Figure 1: The shape and Dimensions (in cm) of the generalized aircraft model

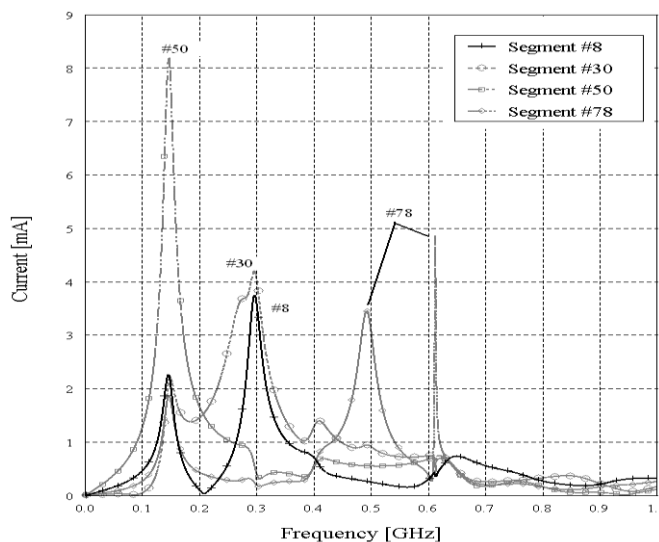
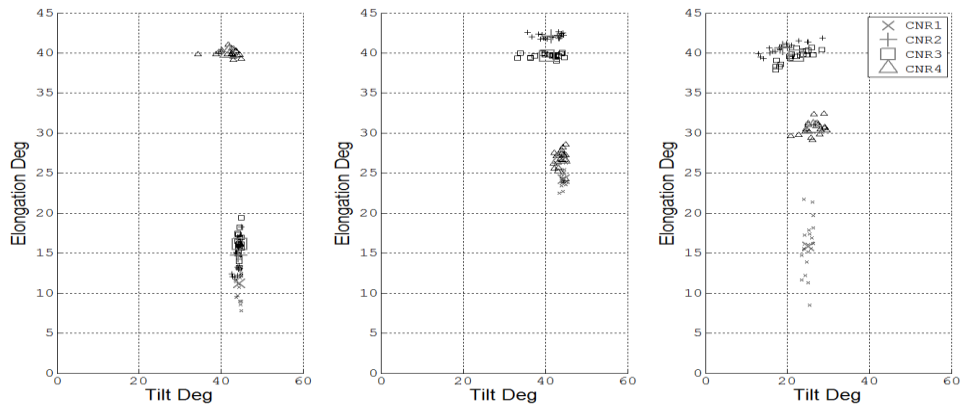


Figure 2: Current-frequency responses of the selected segments belonging to the nose (#8), wing(#30), mid(#50), and tail stabilizer (#78), respectively.

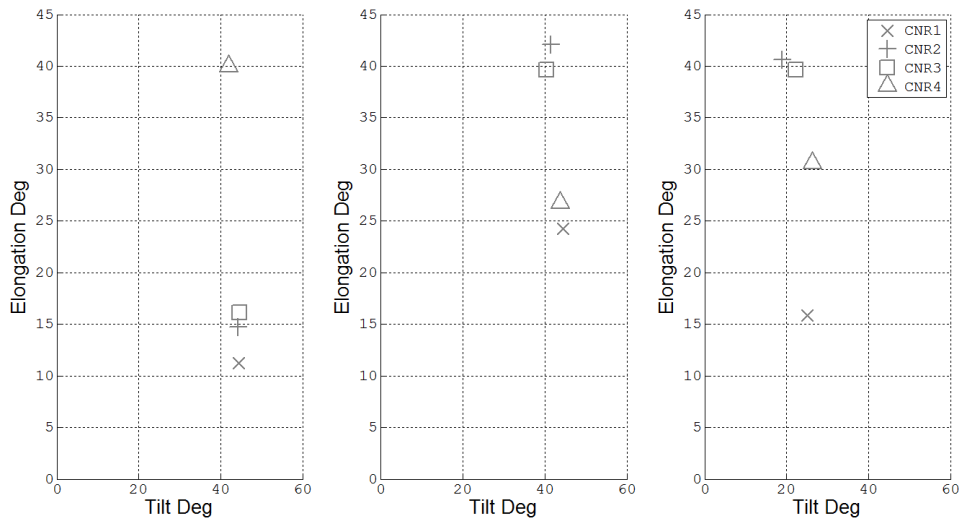


(a) Target A

(b) Target B₄₅

(c) Target B₂₀

Figure 3: Feature space formed by Elongation-Tilt with pools of targets A & B observations under SNR of 5dB and along all four resonances



(a) Target A

(b) Target B₄₅

(c) Target B₂₀

Figure 4: The estimated Elongation-Tilt scatter plot for A & B targets along all four resonances

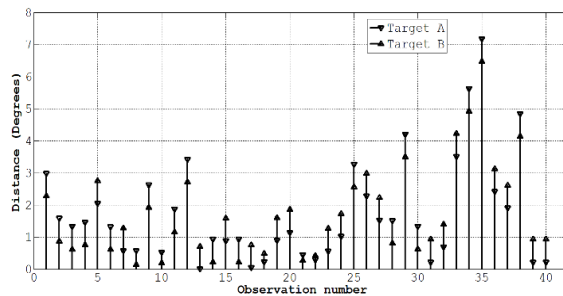


Figure 5: A stemplot of the training-test distances. Based on symmetry-fundamental resonance feature at 5dB SNR setup